FIBRES & TEXTILES in Eastern Europe
sciendo
FIBRES & TEXTILES in Eastern Europe
Research Article • DOI: 10.2478/ftee-2024-0018 FTEE • 32(2) • 2024 • 51–56

Study on Viscoelastic Poisson's Ratio of Nonwovens

Li Yong[1], Kou Yuhang[1], Xia Tengteng[1],
Chu Heying[1]*, Li Lei[1]

[1] Mechanical Engineering College, Tarim University, Alar, Xinjiang, China
* Corresponding author. E-mail: 734841010@qq.com

Abstract
Combined with Laplace transform and creep stress conditions, an accurate expression of the viscoelastic Poisson's ratio calculated from the transverse strain and relax modulus is derived. From creep and relax tests data, Prony series of the transverse strain and relax modulus of nonwovens with time were obtained, and the time-varying curve of the viscoelastic Poisson's ratio of nonwovens was simulated by 1stOpt software. The method proposed can effectively obtain the viscoelastic Poisson's ratio of nonwovens and provide a reference value for calculating mechanical indexes involved in its subsequent production and processing.

Keywords
nonwovens, Poisson's ratio, viscoelasticity, creep, relax, calculation.

1. Introduction

Poisson's ratio is one of the important indexes to measure the mechanical properties of materials, and its accurate measurement is extremely important for processing [1] (2008). Several researchers have studied the Poisson's ratio of knitted fabrics, woven fabrics, nonwovens, etc., but most of them consider fabrics as the elastic material, that is the Poisson's ratio is considered to be a constant. The Poisson's ratio of viscoelastic materials generally shows a correlation with temperature and time. If assumed to be a constant, it will cause a large error in the related stress analysis and strength calculation [2] (2018). With the development of the textile industry, the production and usage of nonwovens have increased year by year, and research on the mechanical properties of nonwovens has gradually received attention. We found that nonwovens had typical viscoelastic properties by means of a tensile test. As one of the basic mechanical parameters of materials, accurate determination of the viscoelastic Poisson's ratio of nonwovens is essential.

At present, there are many studies on the viscoelastic Poisson's ratio of materials, but the study on textile materials has not yet been seen. Lakes R S and Wineman A [3] (2006) conducted a theoretical analysis of the Poisson's ratio in linear viscoelastic solids and found that the viscoelastic Poisson's ratio is a function of the loading time, but does not necessarily increase monotonically with time. In order to analyze the Poisson's ratio and creep compliance of asphalt concrete mixture, Lee and Kim [4] (2009) derived analytical algorithms to determine it in time- and frequency-domain and verified it by means of an indirect tension test. Penava Ž et al. [5] (2017) determined the breaking properties and the Poisson's ratio of woven fabrics with different raw material compositions by uniaxial testing, where the Poisson's ratio of cotton fabrics was higher than that of wool fabrics at the same extended condition, with the Poisson's ratio increasing nonlinearly and decreasing after having reached the peak value. Hoshino Y et al. [2] (2018) proposed a two-dimensional digital image correlation to directly measure the Poisson's ratio in a dynamic viscoelastic test and verified it by testing the material properties of epoxy resin.

Based on the theory of viscoelastic mechanics, this paper established the expression of the viscoelastic Poisson's ratio, combined with creep and relax tests to determine the material tensile index, and accurately calculated the viscoelastic Poisson's ratio of nonwovens, providing a reference for measurement of the Poisson's ratio of textile materials.

2. Analytical Model

The conventional elastic Poisson's ratio *n* is defined as

$$\nu = -\varepsilon_x/\varepsilon_y \tag{1}$$

where e_x and e_y are the transverse and longitudinal strains of the material.

Nonwoven is a typical viscoelastic material, *n* as an indirect characteristic of the structure of the material and the mechanism of its deformation. Generally speaking, the transverse deformation response lags the longitudinal, namely, the change of e_x is caused by e_y. The Poisson's ratio of nonwovens is difficult to obtain due to the lack of testing techniques. Therefore, the accurate Poisson's ratio *n* cannot be calculated directly from the values of e_x and e_y.

Based on the extended elastic-viscoelastic correspondence principle, the time-dependent viscoelastic Poisson's ratio *n*(*t*) relationship of a viscoelastic material subjected to constant uniaxial stress, *n*(*t*) can be expressed as

$$\nu(t) = -\varepsilon_x(t)/\varepsilon_y(t) \tag{2}$$

where $e_x(t)$, $e_y(t)$ are respectively time functions of the transverse and longitudinal strain.

Type	Manufacturer	Material	Area density, g/m²	Thickness, mm	Width of package,mm	Web forming method	Bonding method
PP30	Jialianda Nonwovens Co., Ltd	Polypropylene	30	1.63	143	Spun-laid	Hot pressing
PLA30	Smartwin International Group Co., Ltd	Polylactice acid	30	1.11	1800	Carding web	Carding
PET30	Smartwin International Group Co., Ltd	Polyethylene terephthalate	30	0.95	1800	Spun-laid	Hot pressing
PA20	Smartwin International Group Co., Ltd	Polyamide	20	0.80	1800	Spun-laid	Hot pressing
PA30	Smartwin International Group Co., Ltd	Polyamide	30	1.08	1800	Spun-laid	Hot pressing
PA40	Smartwin International Group Co., Ltd	Polyamide	40	1.28	1800	Spun-laid	Hot pressing

Table 1. Properties and parameters of samples

The Poisson's ratio *n*(*t*), which characterizes the response of the transverse strain $e_x(t)$ to the longitudinal strain $e_y(t)$ under a static tensile load, is a memory function of transverse deformation.

For linear viscoelastic materials, taking Laplace transform on the Eq. 2, the Poisson's ratio *n*(*s*) is defined as

$$\bar{v}(s) = -\bar{\varepsilon}_x(s)/\bar{\varepsilon}_y(s) \qquad (3)$$

where *s* is transform variable, the longitudinal strain $\bar{\varepsilon}_y(s) = \bar{\sigma}_y(s)/\bar{E}(s)$, the longitudinal stress $\bar{\sigma}_y(s) = \sigma_0/s$ in the creep test, "–" on the symbol denotes the Laplace operator.

Here Eq. 3 can be written as

$$\bar{v}(s) = -\bar{\varepsilon}_x(s)s\bar{E}(s)/\sigma_0 \qquad (4)$$

where s_0 is the creep tensile stress, *E* is the tensile relax modulus.

Using the convolution theorem to calculate the inverse Laplace transform of Eq. 4, can be obtained

$$v(t) = -\frac{1}{\sigma_0}\int_0^t E(t-\tau)\varepsilon_x(\tau)\mathrm{d}\tau \qquad (5)$$

Using Eq. 5, an accurate value of the viscoelastic Poisson's ratio *n*(*t*) can be obtained from the measured values of $e_x(t)$ and *E*(*t*), which is the theoretical basis for indirectly test of the viscoelastic Poisson's ratio.

Let $e_x(t)$ and *E*(*t*) be the Prony series, as follows

$$\begin{cases} \varepsilon_x(t) = \varepsilon_{xe} + \sum_{i=1}^{m} \varepsilon_{xi} exp(-t/\tau_i) \\ E(t) = E_e + \sum_{j=1}^{n} E_j exp(-t/\tau_j) \end{cases} \qquad (6)$$

where *m* and *n* are the order of the Prony series, e_{xe} the final strain, e_{xi} and t_i express the strain and creep time of each order, E_e gives the equilibrium modulus, E_j and t_j indicate the relax modulus and relax time of each order.

Substituting Eq. 6 into Eq. 5 and rearranging, the accurate expression of the viscoelastic Poisson's ratio of material can be obtained

$$v(t) = -\frac{1}{\sigma_0}[E_e \sum_{i=1}^{m} \varepsilon_{xi}(exp(-t/\tau_i) - 1) + \sum_{i=1}^{m}\sum_{j=1}^{n} \frac{\varepsilon_{xi}E_j\tau_j}{\tau_j - \tau_i}(exp(-t/\tau_i) - exp(-t/\tau_j))] \qquad (7)$$

3. Experiments

3.1. Material

The work is based on six kinds of nonwovens; their properties and parameters are shown in Table 1. The surface morphology of nonwovens was measured by means of the microscopy technique (Figure 1); their surface morphology is shown in Figure 2. The PP, PET, and PA nonwovens are the melt-blown nonwoven mats, the PLA nonwovens are the carding web, and their thermal bonding is fiber-fiber bonding by the hot press, The square hot pressing points are distributed on the nonwoven surface.

Considering the thickness of the sample is small, ignoring the stress and strain components in the thickness direction of the nonwovens, only the two-dimensional plane Poisson's ratio of the nonwovens is discussed. Because the selected nonwovens had no warp or weft, this paper considers them to be a plane isotropic material.

3.2. Creep Test

Under standard laboratory conditions (20°C±2°C, 65%±4% relative humidity), the upper and lower ends of the sample were clamped with fixtures, suspended, and a longitudinal load applied. The sample size was 300 mm×70 mm and the clamping distance 200 mm. To avoid the influence of the edge curling, the measurement position was 10 mm from the edge; that is the measurement width was 50 mm. To prevent the nonwovens

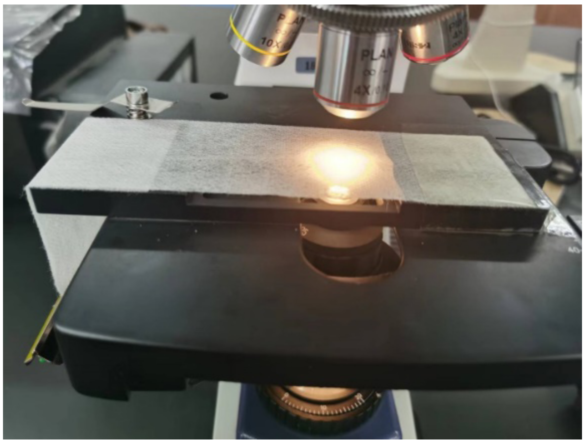

Fig. 1 Measurement of surface morphology of nonwovens

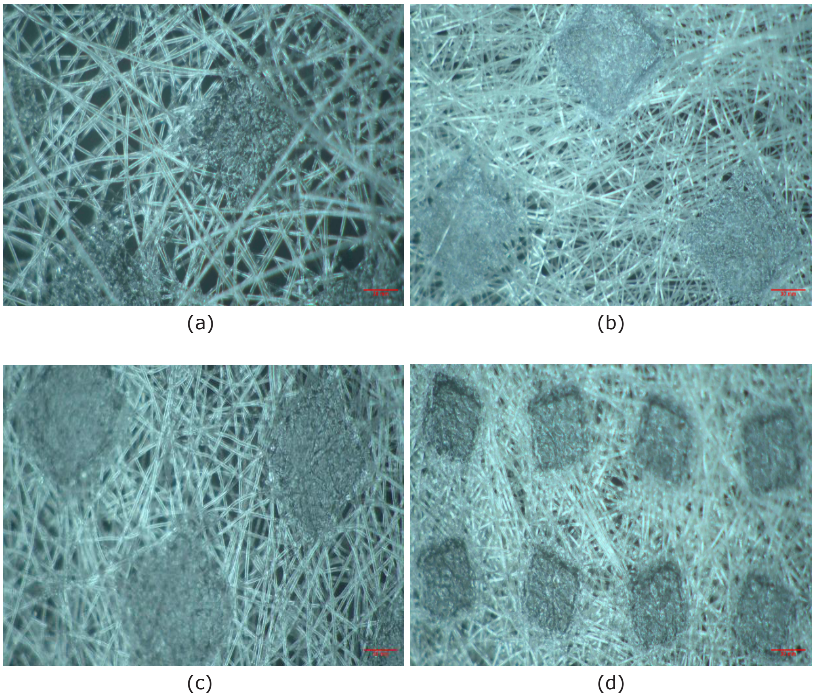

Fig. 2 Photos of surface morphology of nonwovens, (a) PP30, (b) PLA30, (c) PET30, (d) PA30

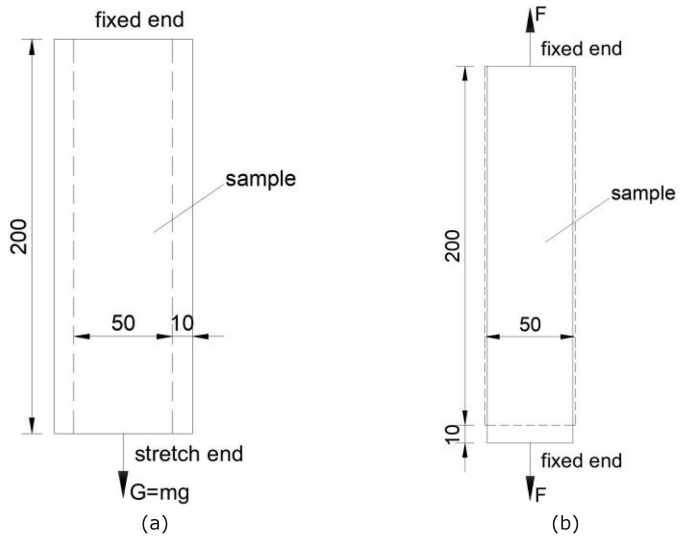

Fig. 3 Schematic diagram of creep and relax tests: (a) creep test, (b) relax test

from being structurally damaged and the transverse strain to be measurable, the longitudinal load was determined to be 0.239 MPa (imposed by the lower end fixture and the weight together, 20.7 g for the fixture and 500 g for the weight), and the load was applied instantaneously and lasted 12 h. The testing schematic diagram is shown in Fig. 3(a). The variation in the width at the narrowest point in the middle of the sample with creep time was measured and recorded, for five repetitions and the average value taken. The transverse strain e_x'. was then calculated. Considering the slight necking phenomenon of nonwovens under small load, the e_x - t curve is obtained by taking 0.5e_x' as the equivalent transverse strain e_x.

3.3. Relax Test

The relaxation properties of the nonwovens were tested in the longitudinal direction using a geotextile comprehensive strength testing machine (Wenzhou Darong Textile Instrument Co., Ltd., Zhejiang, China) under standard laboratory conditions (20°C ± 2°C, 65% ± 4% relative humidity). The sample size was 300 mm□50 mm and the clamping distance 200 mm. Test data processing was conducted by the data fitting method based on the Prony series [6] (2011), which comprehensively considers the loading and relax stage of the relax test. The initial strain and loading speed do not affect the calculation results. Considering the test efficiency and avoiding the impact load, the tensile speed was set at 20 mm/min. In order to prevent the nonwovens from being damaged, and the stress to be measurable, the sample was stretched to 0.05 longitudinal strain and then stopped, maintaining the tensile state for 12 h. The testing schematic diagram is shown in Fig. 3(b). The change in the tensile force value with relax time was recorded, from which the tensile stress s, can be calculated and the s - t curve plotted.

4. Results and Discussion

4.1. Creep Test

In the creep test, the relationship between the equivalent transverse strain and time in the creep process is obtained, as shown in Fig. 4.

At the moment of loading, the equivalent transverse strain of PP30, PLA30, and PET30 was about 0.023, 0.01175, and 0.00924, that of PA20, PA30, and PA40 was about 0.0164, 0.00765, and 0.0029, as shown in Fig. 4. The strain at this stage was mainly caused by the elastic deformation of the fibers or fiber web. Subsequently, with the increase of the creep time, the transverse strain gradually increased and approached a constant value, with the strain at this stage attributed to the gradual peeling and slippage of the bonding points between fibers inside the nonwovens.

As the area density increased, the elastic deformation and structural plastic deformation capacity of the PA nonwovens weakened. When the area density was 30 g/m^2, the elastic deformation ability of the nonwovens from high to low in turn was PP30, PLA30, PA30, and PET30.

Using the Levenberg-Marquardt optimization algorithm to fit the curve of the creeping stage (after the instantaneous strain), the Prony series with order 6 expression of the equivalent transverse strain $e_x(t)$ of nonwovens is obtained.

$$\varepsilon_x(t) = \varepsilon_{xe} + \sum_{i=1}^{m=6} \varepsilon_{xi} exp(-t/\tau_i) \quad (8)$$

Table 2 shows the Prony series with order 6 expression of the equivalent transverse strain of PA, PP, PLA, and PET nonwovens. All parameter values are fitting results, the correlation coefficients between the fitted and measured values are all higher than 0.98, indicating a better fitting effect.

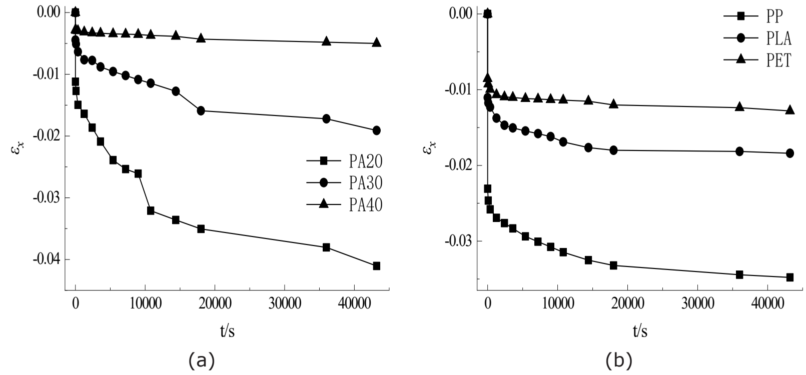

Fig. 4 Strain-time curve of creep test: (a) PA20, PA30 and PA40, (b)PP30, PLA30, and PET30

Type	Regression equation
PP30	$\varepsilon_x(t)$=4.42628+1.09253e$^{-t/32028.50978}$+0.73885e$^{-t/282.31417}$+ 0.58798e$^{-t/3771.29624}$+1.60838e$^{-t/57.29553}$+ 0.52102e$^{-t/1346.1015}$+7.18362e$^{-t/7.14774}$
PLA30	$\varepsilon_x(t)$=-0.01837+0.00203e$^{-t/690.82678}$+0.00354e$^{-t/1.71985}$+ 0.00254e$^{-t/3345.76762}$+0.00813e$^{-t/1.76406}$+ 0.00076e$^{-t/17688.93783}$+0.00137e$^{-t/159.68997}$
PET30	$\varepsilon_x(t)$=-0.01317+0.00902e$^{-t/1.90676}$+0.00209e$^{-t/29409.01145}$+ 0.00004e$^{-t/2.15781}$+0.00001e$^{-t//23847.32555}$+ 0.00069e$^{-t/29.86732}$+0.00133e$^{-t/255.54712}$
PA20	$\varepsilon_x(t)$=-0.04475+0.00433e$^{-t/43199.94444}$+9.88×10^{-18}e$^{-t/1118.18378}$+ 0.01821e$^{-t/1654.64907}$+0.00861e$^{-t/43199.93206}$+ 0.00334e$^{-t/7.33281}$+0.01027e$^{-t/1.95681}$
PA30	$\varepsilon_x(t)$=-0.01967+0.00378e$^{-t/802.57842}$+2.29×10^{-13} e$^{-t/15657.97923}$+ 0.0024e$^{-t/10.92507}$+0.00566e$^{-t/23940.20253}$+ 0.00422e$^{-t/13740.79532}$+0.0036e$^{-t/1.19744}$
PA40	$\varepsilon_x(t)$=-0.00554+0.00184e$^{-t/35871.37391}$+4.91×10^{-12}e$^{-t/23381.26005}$+ 0.00289e$^{-t/1.47535}$+0.00029e$^{-t/12560.94798}$+ 1.15×10^{-21}e$^{-t/29276.85456}$+0.00052e$^{-t/527.90410}$

Table 2. Prony series with order 6 expression of the equivalent transverse strain

4.2. Relax Test

In the relax test, the relationship between longitudinal stress and time in the stress relax process of the nonwovens was obtained, as shown in Fig. 3.

In the initial relax stage, the stress of the sample decreased sharply, as shown in Fig. 3. This shows that the nonwovens had strong relax characteristics, and the stress change at this stage was mainly caused by fiber straightening and slippage. Subsequently, the downward trend of stress gradually slowed and was nearly a constant value, with the stress change at this stage attributed to the stress relaxation of the fibers after straightening. At a tensile strain rate of 5%, the higher the area density of the nonwovens, the greater the tensile stress and the greater the residual stress after stress attenuation. At an area density of 30 g/m^2, the residual stress from high to low in turn is PET30, PP30, PLA30, and PA30. This reflects that the higher the material density and the higher the tensile resistance index, the stronger the corresponding tensile resistance.

Using the data fitting method based on the Prony series and the Levenberg-Marquardt optimization algorithm, the curve of the relax stage was fitted, and the Prony series with order 6 expression of the relax modulus $E(t)$ of the nonwovens was obtained

$$E(t) = E_e + \sum_{j=1}^{n=6} E_j exp\left(-t/\tau_j\right) \quad (9)$$

Table 3 shows the Prony series with order 6 expression of the relax modulus of PA, PP, PLA, and PET nonwovens. All parameter values are fitting results, the correlation coefficients between the fitted and measured values being all higher than 0.98, indicating a better fitting effect.

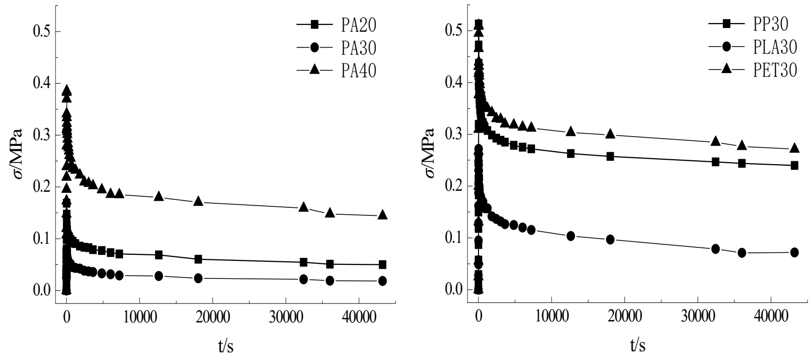

(a) (b)

Fig. 3 Stress-time curve of relax test,(a) PA20, PA30 and PA40, (b)PP30, PLA30 and PET30

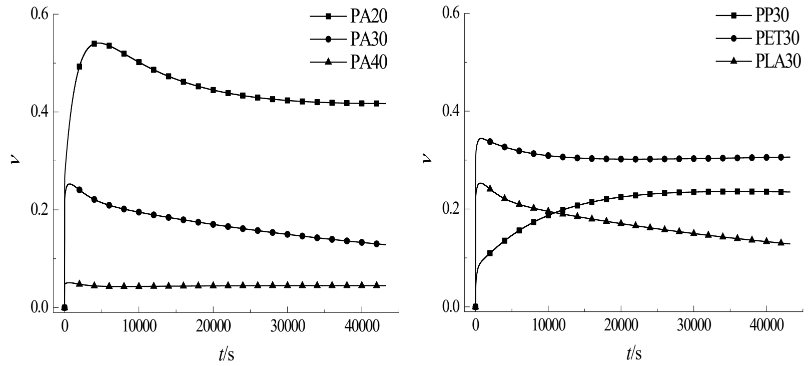

(a) (b)

Fig. 4 Poisson's ratio-time curve: (a) PA20, PA30 and PA40, (b)PP30, PLA30 and PET30

Type	Regression equation
PP30	$E(t)=4.42628+1.09253e^{-t/32028.50978}+0.73885e^{-t/282.31417}+0.58798e^{-t/3771.29624}+1.60838e^{-t/57.29553}+0.52102e^{-t/1346.1015}+7.18362e^{-t/7.14774}$
PLA30	$E(t)=0.72456+4.52\times10^{-14}e^{-t/20545.52934}+1.24187e^{-t/2137.01999}+1.43\times10^{-13}e^{-t/36360.07692}+7.56\times10^{-14}e^{-t/9155.68766}+1.77333e^{-t/43199.70987}+9.20\times10^{-13}e^{-t/16839.05726}$
PET30	$E(t)=5.38462+1.64\times10^{-16}e^{-t/453.42766}+1.20874e^{-t/6652.87856}+1.22\times10^{-13}e^{-t/23242.29474}+1.70\times10^{-8}e^{-t/32347.22098}+4.75E^{-7}e^{-t/1705.50865}+0.57320e^{-t/14404.62676}$
PA20	$E(t)=0.90989+0.89126e^{-t/12247.20516}+7.23\times10^{-7}e^{-t/33414.44565}+1.52\times10^{-6}e^{-t/8424.74793}+2.56\times10^{-13}e^{-t/93。12918}+2.93\times10^{-8}e^{-t/18919.63773}+0.01144e^{-t/15146.15837}$
PA30	$E(t)=0.31736+0.18224e^{-t/20190.21103}+0.48432e^{-t/2192.37282}+1.30\times10^{-17}e^{-t/34546.26469}+6.98\times10^{-5}e^{-t/24365.33458}+0.00039e^{-t/25031.94717}+0.12488e^{-t/17679.49483}$
PA40	$E(t)=2.49469+0.00083e^{-t/9403.58163}+1.69301e^{-t/2187.80999}+2.15\times10^{-9}e^{-t/22263.27476}+0.01963e^{-t/2349.39762}+1.20932e^{-t/34067.64849}+0.00011e^{-t/7157.69109}$

Table 3. Prony series with order 6 expression of the relax modulus

4.3. Viscoelastic Poisson's Ratio Calculation

After the Prony series with order 6 of the transverse strain $e_x(t)$ and relax modulus $E(t)$ of the nonwovens are known (correlation coefficients R are greater than 0.98), the fitting parameters are substituted into Eq. 7. 1stOpt software was used to compile a calculation program, with the calculation step t = 1 s. According to the calculation result, using Origin software to draw the curve of Eq. 7, the relationship between the Poisson's ratio and time under the creep condition of the nonwovens, was obtained as shown in Fig. 4.

The viscoelastic Poisson's ratio of the nonwovens has an obvious time effect, as shown in Fig. 4. In the creep process, with the increase of the loading time, the Poisson's ratio of the nonwovens gradually increases from 0 to its peak, then gradually decreases, and tends towards equilibrium. Therefore, the peak value of Poisson's ratio can be regarded as the initial viscoelastic Poisson's ratio of the nonwovens. Poisson's ratio is a value that gradually approaches a constant value from a peak value over time. Comparing the Poisson's ratio of each sample, it is found that as the area density increased, the Poisson's ratio of the PA nonwovens decreased. At a 30 g/m^2 area density, the Poisson's ratio of nonwovens from high to low in turn is PLA30, PA30, PP30, and PET30, which are not the same value. The Poisson's ratio of non-woven fabrics is closely related to their material structure and mechanical properties. The viscoelastic Poisson's ratio of nonwovens obtained in this paper is in the normal Poisson's ratio range (0-0.5). It accords with the situation that the Poisson's ratio of most materials is about 1/3 [7] (2000). The convergence value of the Poisson's ratio of PP30 and PET30 (n_{PP30} = 0.25,n_{PET30} = 0.32) is similar to the elastic Poisson's ratio of thermally bonded polypropylene nonwovens (point bonded) obtained by Gao [8] (2014). The existing discrepancy may be due to different fabric specifications, production processes, etc., but it still has a specific reference value. Then, the changing trend gradually slows until nearly a constant value.

5. Conclusion

The Poisson's ratio of viscoelastic materials cannot be assumed to be constant but a time-dependent function. Based on the viscoelastic properties of nonwovens, this paper deduces an equivalent calculation method for Poisson's ratio using the transverse strain $ex(t)$ and relax modulus $E(t)$. The Prony series fit the creep and relax test data to obtain $ex(t)$ and $E(t)$. Then, the relationship between Poisson's ratio and the time of the nonwovens is calculated using 1stOpt software. It is found that the Poisson's ratio of the nonwovens gradually increases from 0 to its peak, then gradually decreases and tends towards equilibrium. The result is in the conventional Poisson's ratio range and agrees well with related studies. The method describes how it can easily calculate the viscoelastic Poisson's ratio of textile materials (such as nonwovens) and provide a reference value for calculating mechanical indexes involved in subsequent production and processing.

References

1. Mott PH., Dorgan JR., Roland CM. The bulk modulus and Poisson's ratio of "incompressible" materials. *Journal of Sound and Vibration* 2008; 312(4-5): 572-575.
2. Hoshino Y, Tamai K, Zhang YL and Satoru Y. Direct measurement and master curve construction of viscoelastic Poisson's ratio with digital image correlation. *Strain* 2018; 54:e12294.
3. Lakes RS, Wineman A. On Poisson's ratio in linearly viscoelastic solids. *Journal of Elasticity* 2006; 85(1): 45-63.
4. Lee HS, Kim J. Determination of Viscoelastic Poisson's Ratio and Creep Compliance from the Indirect Tension Test. *Journal of Materials in Civil Engineering* 2009; 21(8): 416-425.
5. Penava Ž, Šimić Penava D, Knezić Ž. Influence kinds of materials on the Poisson's ratio of woven fabrics. *Tehnički glasnik* 2017; 11(3): 101-106.
6. Xu JS, Jin YT, Zheng J and Han B. Acquisition of the relax modulus of Composite solid propellant. *Chinese Journal of Explosives & Propellants* 2011; 34(5): 58-62.
7. Alderson KL, Fitzgerald A, Evans KE. The strain dependent indentation resilience of auxetic microporous polyethylene. *Journal of Materials Science* 2000; 35(16): 4039-4047.
8. Gao XP, Song QJ. Measurement of Poisson's ratio of nonwoven geotextile based on image processing technology. *Technical Textiles* 2014; 32(12): 35-38.